Calculations of antiproton-nucleus quasi-bound states based on the Paris $\bar{N}N$ potential.

Jaroslava Hrtánková

Nuclear Physics Institute, Řež, Czech Republic

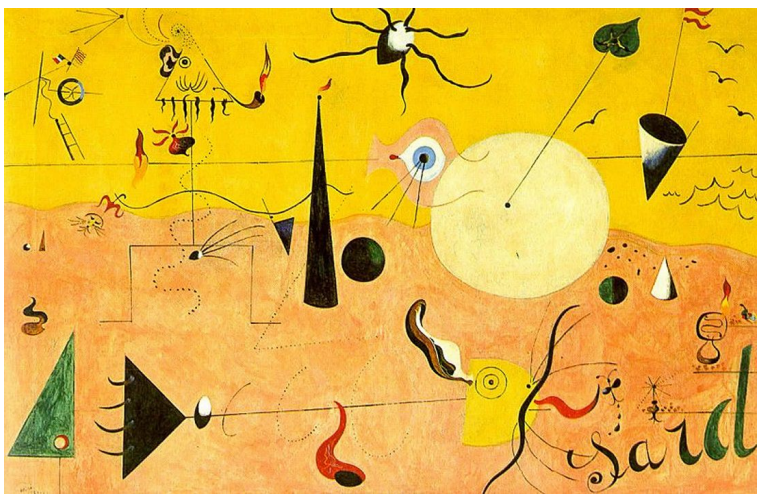

FAIRNESS 2017, May 28 - June 3, 2017, Sitges, Catalunya

Introduction

- study of $\bar{p}$ interaction with selected nuclei:
  - behavior of $\bar{p}$ in the nuclear medium
  - $\bar{p}$ absorption in a nucleus
  - testing models of (anti)baryon–baryon interactions as well as models for nuclear structure calculations
- previous study *I.N. Mishustin et al., Phys. Rev. C 71 (2005)*
  - possibility of long living $\bar{p}$ in the nuclear medium?
- the BES collaboration observed a near-threshold enhancement in the $\bar{p}p$ mass spectrum

  J. Z. Bai et al. (BES Collaboration), Phys. Rev. Lett. 91 (2003) 022001.
- knowledge of $\bar{p}$–nucleus interaction for future experiments (PANDA@FAIR)

Model

- $\bar{p}$ binding energies and widths are obtained by solving the Dirac equation

$$[-i\vec{\alpha}\vec{\nabla} + \beta m_{\bar{p}} + V_{\text{opt}}]\psi_{\bar{p}} = \epsilon_{\bar{p}}\psi_{\bar{p}},$$

  $m_{\bar{p}}$ is the $\bar{p}$ mass, V_{opt} is a complex optical potential, $\epsilon_{\bar{p}} = -B_{\bar{p}} - i\frac{\Gamma_{\bar{p}}}{2}$, $(B > 0)$

- the S-wave optical potential constructed in a '$t\rho$' form

$$2E_{\bar{p}}V_{\text{opt}} = -4\pi\frac{\sqrt{s}}{m_N}\left(F_0\frac{1}{2}\rho_p + F_1\left(\frac{1}{2}\rho_p + \rho_n\right)\right) \ ,$$

  where $E_{\bar{p}} = m_{\bar{p}} - B_{\bar{p}}$, F_0 and F_1 – isospin 0 and 1 scattering amplitudes, ρ_p (ρ_n) is the proton (neutron) density distribution calculated in the RMF model

Scattering amplitudes

- free-space scattering amplitudes $\rightarrow$ microscopic Paris $\bar{N}N$ potential constrained by scattering and antiproton atom data
  (*B. El-Bennich, M. Lacombe, B. Loiseau, S. Wycech, Phys. Rev. C 79 (2009) 054001)*
- the optical potential based on Paris amplitudes was recently confronted with the $\bar{p}$-atom data and low energy $\bar{p}$ scattering off nuclei
  (*E. Friedman, A. Gal, B. Loiseau, S. Wycech, NPA 934 (2015) 101)*

Scattering amplitudes

- in-medium S-wave amplitudes F_0 and F_1 obtained from free-space amplitudes by multiple scattering approach (WRW)
  (*T. Wass, M. Rho, W. Weise, NPA 617 (1997) 449)*

$$F_1 = \frac{f_{\bar{p}n}(\delta\sqrt{s})}{1 + \frac{1}{4}\xi_k \frac{\sqrt{s}}{m_N} f_{\bar{p}n}(\delta\sqrt{s})\rho}\,, F_0 = \frac{[2f_{\bar{p}p}(\delta\sqrt{s}) - f_{\bar{p}n}(\delta\sqrt{s})]}{1 + \frac{1}{4}\xi_k \frac{\sqrt{s}}{m_N}[2f_{\bar{p}p}(\delta\sqrt{s}) - f_{\bar{p}n}(\delta\sqrt{s})]\rho}\,,$$

where $\delta\sqrt{s} = \sqrt{s} - E_{\text{th}}$, $\xi_k = \frac{9\pi}{p_f^2}\, 4\int_0^\infty \frac{dt}{t} \exp(iqt) j_1^2(t)$ and $q = \frac{1}{p_f}\sqrt{E_{\bar{p}}^2 - m_{\bar{p}}^2}$

In-medium Paris S-wave amplitudes

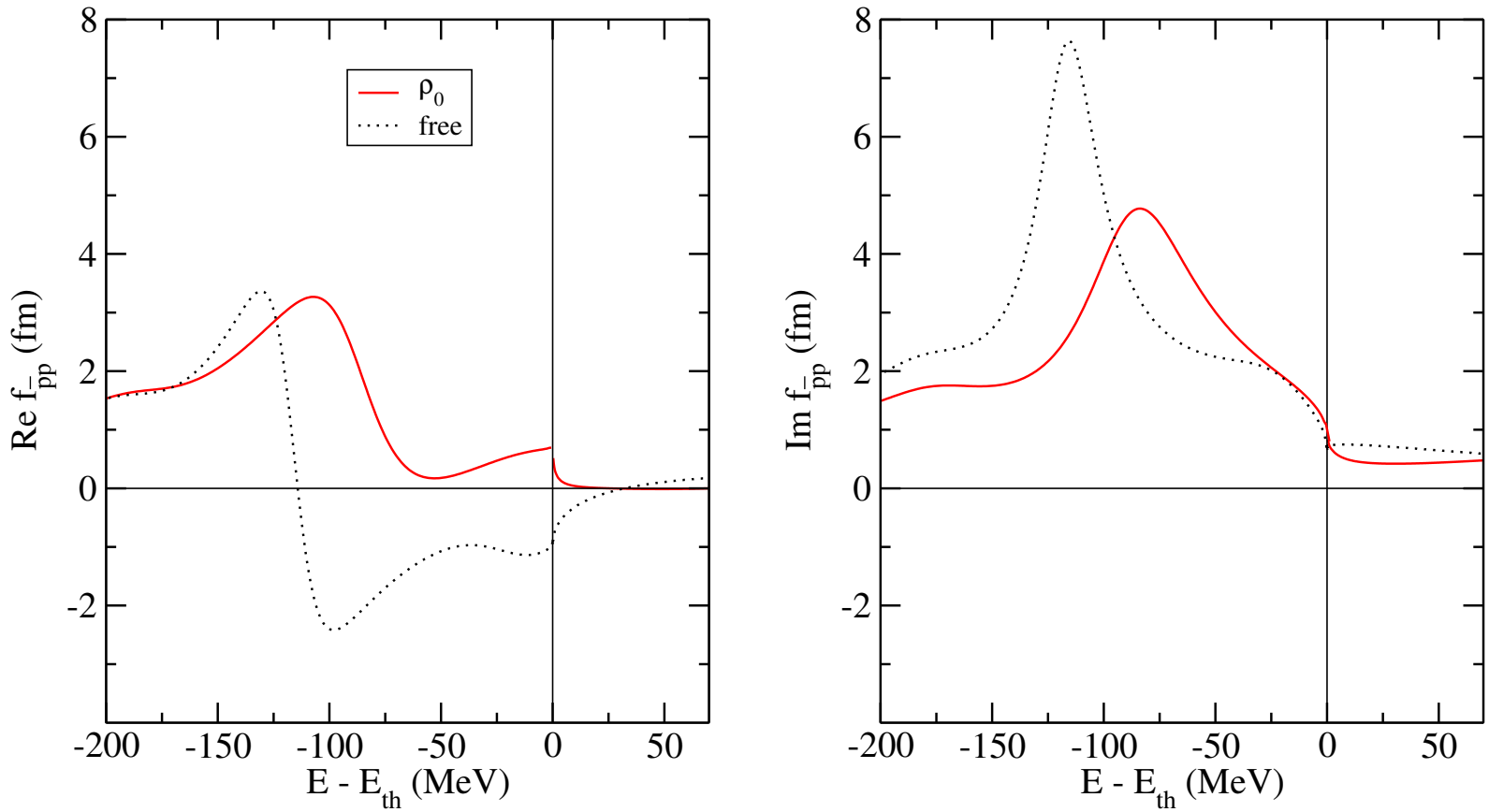

Fig.1: Energy dependence of the Paris 09 $\bar{p}p$ S-wave amplitudes: Pauli blocked amplitude for $\rho_0 = 0.17$ fm^{-3} (solid lines) compared with free-space amplitude (dotted lines).

In-medium Paris S-wave amplitudes

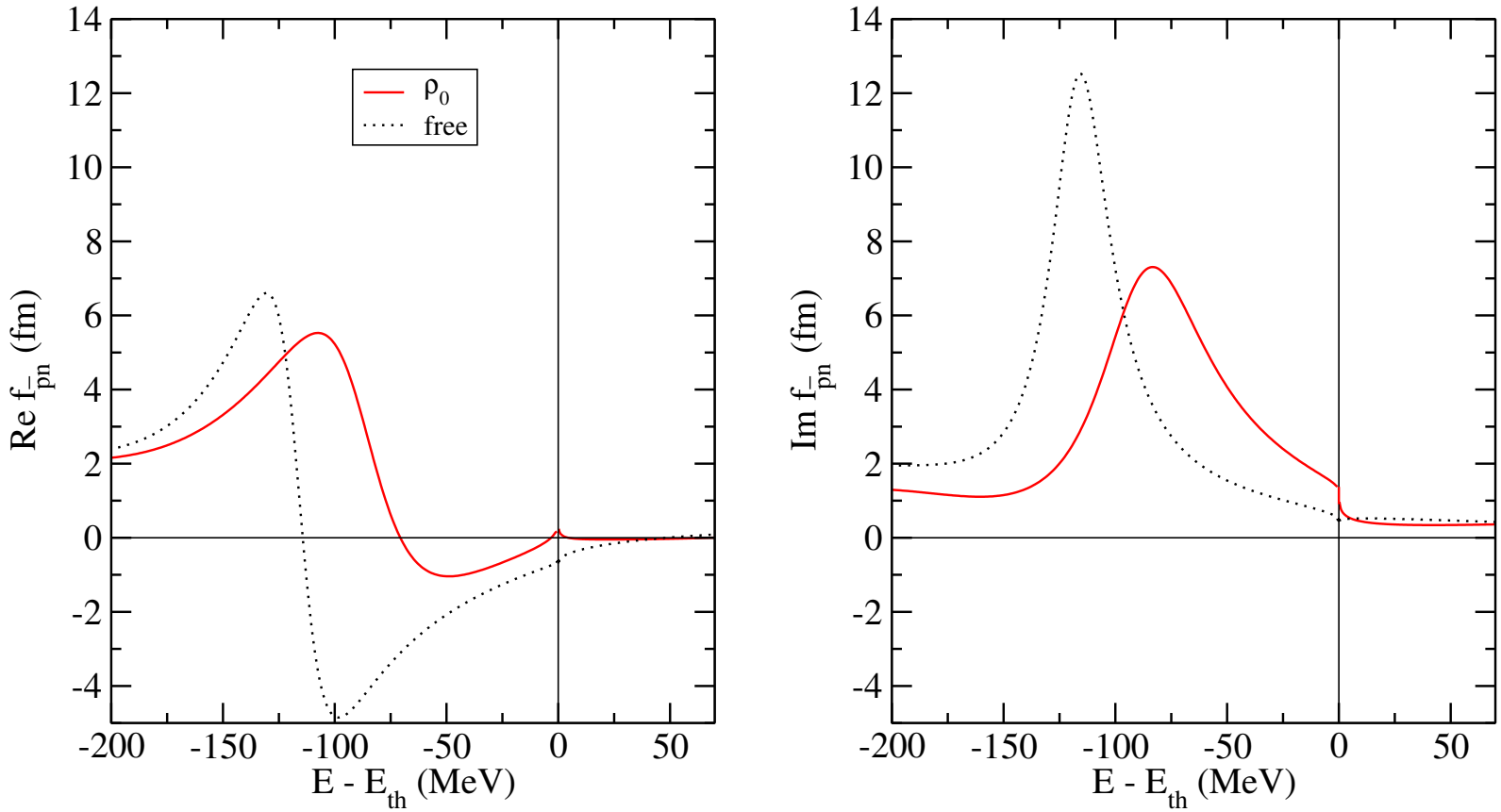

Fig.2: Energy dependence of the Paris 09 $\bar{p}n$ S-wave amplitudes: Pauli blocked amplitude for $\rho_0 = 0.17$ fm^{-3} (solid lines) compared with free-space amplitude (dotted lines).

Previous calculations – RMF approach

- Nucleons – Dirac fields interacting via the exchange of meson fields
- Dirac equation for nucleons and antiproton

$$[-i\vec{\alpha}\vec{\nabla} + \beta(m_j + S_j) + V_j]\psi_j^\alpha = \epsilon_j^\alpha \psi_j^\alpha \ , \quad j = N, \bar{p} \ ,$$

$$S = g_{\sigma j}\sigma, \quad V_j = g_{\omega j}\omega_0 + g_{\rho j}\rho_0\tau_3 + e_j\frac{1+\tau_3}{2}A_0 \ ,$$

- Klein-Gordon equations for meson fields

$$\begin{aligned}
(-\triangle + m_\sigma^2)\sigma &= -g_{\sigma N}\rho_S - g_{\sigma\bar{p}}\rho_{S\bar{p}} \\
(-\triangle + m_\omega^2)\omega_0 &= g_{\omega N}\rho_V + g_{\omega\bar{p}}\rho_{V\bar{p}} \\
(-\triangle + m_\rho^2)\rho_0 &= g_{\rho N}\rho_I + g_{\rho\bar{p}}\rho_{I\bar{p}} \\
-\triangle A_0 &= e\rho_p + e_{\bar{p}}\rho_{\bar{p}}.
\end{aligned}$$

$\bar{p}$-nucleus interaction

- $NN \to \overline{N}N$ interaction – G-parity transformation $\hat{G} = \hat{C}e^{i\pi I_2}$

$$g_{\sigma\bar{p}} = g_{\sigma N}, \quad g_{\omega\bar{p}} = -g_{\omega N}, \quad g_{\rho\bar{p}} = g_{\rho N}$$

- G-parity valid for the long and medium range $\bar{N}N$ potential
  $\to$ 750 MeV deep $\bar{p}$ potential in the nucleus
- Nuclear medium + short range interactions – possible deviations from the G-parity
- Antiprotonic atoms and $\bar{p}$ scattering off nuclei at low energies
  $\to$ ReV$_{\bar{p}} \sim 100 - 300$ MeV deep
- Reduced $\bar{p}$ coupling constants

$$g_{\sigma\bar{p}} = \xi\, g_{\sigma N}, \quad g_{\omega\bar{p}} = -\xi\, g_{\omega N}, \quad g_{\rho\bar{p}} = \xi\, g_{\rho N} \ ,$$

where parameter $\xi = 0.2 - 0.3$

$\bar{p}$ absorption

- $\bar{p}$–nucleus potential:

$$\mathrm{Re}\,V_{\bar{p}} = \xi\, V_{\mathrm{RMF}}$$

$$\mathrm{Im}\,V_{\bar{p}} = \sum_{channel} f_s(\sqrt{s})\, B_r\, \mathrm{Im}\, b_0\, \rho$$

$$\xi = 0.2,\ \mathrm{Im}\, b_0 = 1.9\ \mathrm{fm}$$

- $\sqrt{s} = m_{\bar{p}} + m_N - B_{\bar{p}} - B_N$

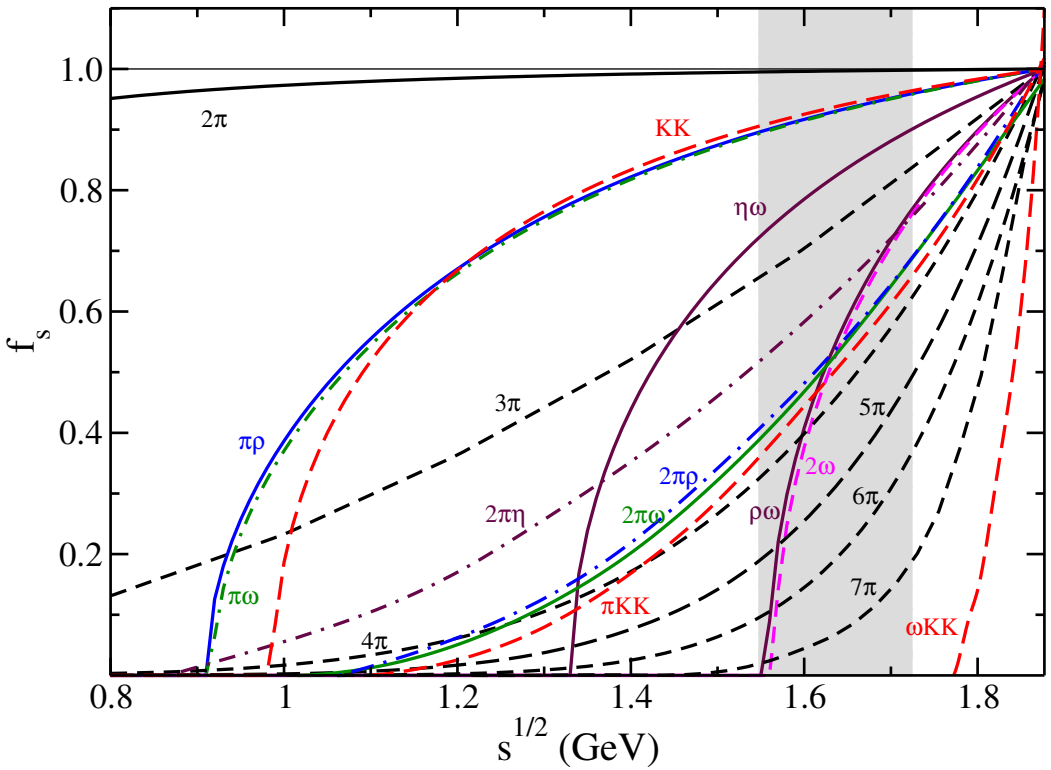

Fig.3: The phase space suppression factor f_s as a function of the center-of-mass energy $\sqrt{s}$.

Energy dependence

- $\bar{p}N$ Paris amplitudes — functions of energy shift $\delta\sqrt{s} = \sqrt{s} - E_{th}$
  $(s = (E_N + E_{\bar{p}})^2 - (\vec{p}_N + \vec{p}_{\bar{p}})^2)$
- CMS frame $\rightarrow \sqrt{s} = m_{\bar{p}} + m_N - B_{\bar{p}} - B_N$ (M)
- $\bar{p}$ absorption in a nucleus $\rightarrow \vec{p}_N + \vec{p}_{\bar{p}} \neq 0$
  (*A. Cieplý, E. Friedman, A. Gal, D. Gazda, J. Mareš, PLB 702, 402 (2011)*)

$$\sqrt{s} = E_{th}\left(1 - \frac{2(B_{\bar{p}} + B_{Nav})}{E_{th}} + \frac{(B_{\bar{p}} + B_{Nav})^2}{E_{th}^2} - \frac{1}{E_{th}} T_{\bar{p}} - \frac{1}{E_{th}} T_{Nav}\right)^{1/2}, \quad \text{(J)}$$

$$T_{Nav} = -\frac{\hbar^2}{2m_N^{(*)}}\triangle, \text{ where } m_N^* = m_N - S_N$$

$$T_{\bar{p}} = -\frac{\hbar^2}{2m_{\bar{p}}^{(*)}}\triangle, \text{ where } m_{\bar{p}}^* = m_{\bar{p}} - \mathrm{Re}V_{\mathrm{opt}}$$

Energy dependence of the $\bar{p}$ potential

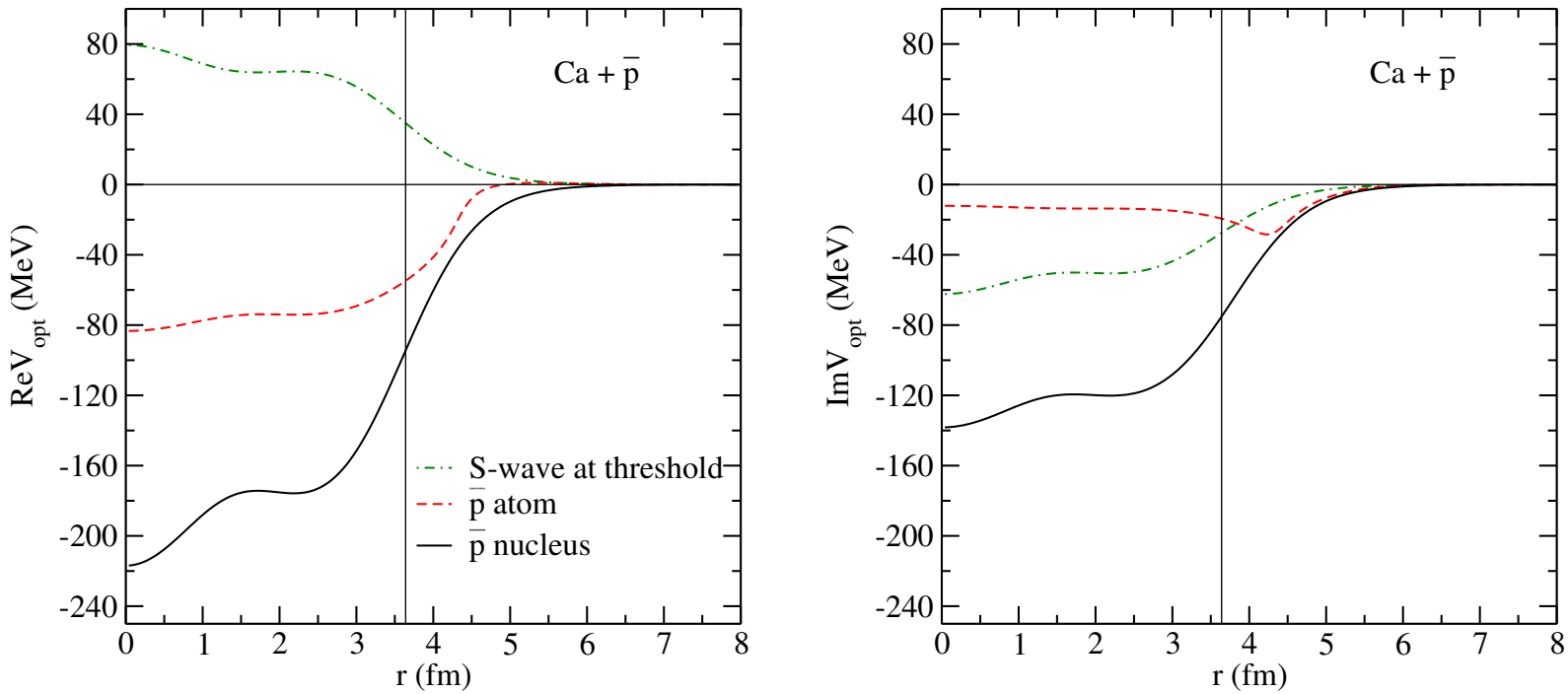

Fig.4: The potential felt by $\bar{p}$ at threshold, in the $\bar{p}$ atom and in the $\bar{p}$ nucleus, calculated for ^{40}Ca+$\bar{p}$ with Paris S-wave amplitudes and static RMF densities.

S-wave Paris potential

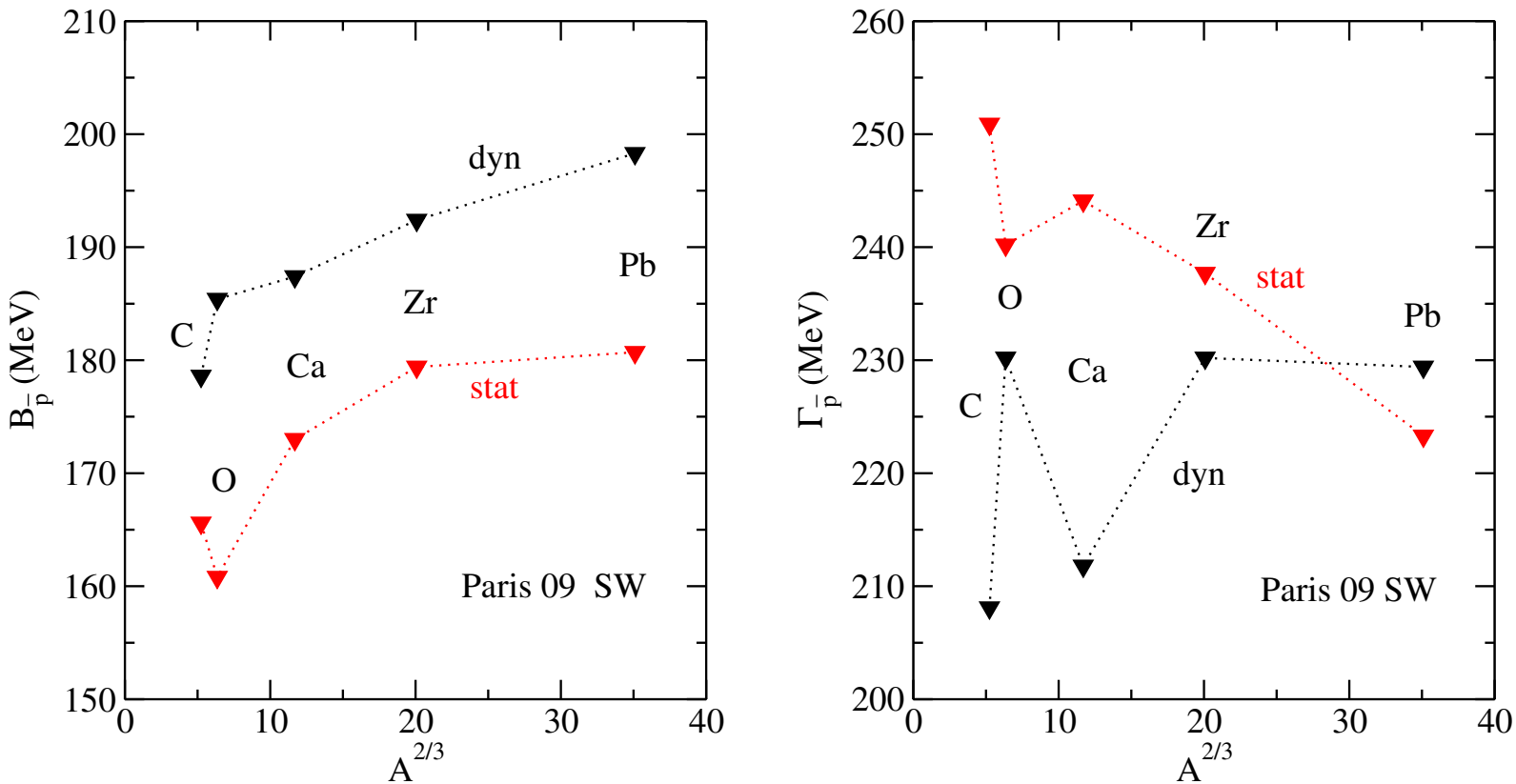

Fig.5: $1s$ $\bar{p}$ binding energies $B_{\bar{p}}$ (left) and widths $\Gamma_{\bar{p}}$ (right) in various nuclei, calculated statically (red) and dynamically (black) with S-wave Paris amplitudes and $\sqrt{s} =$ Jr.

S-wave Paris potential

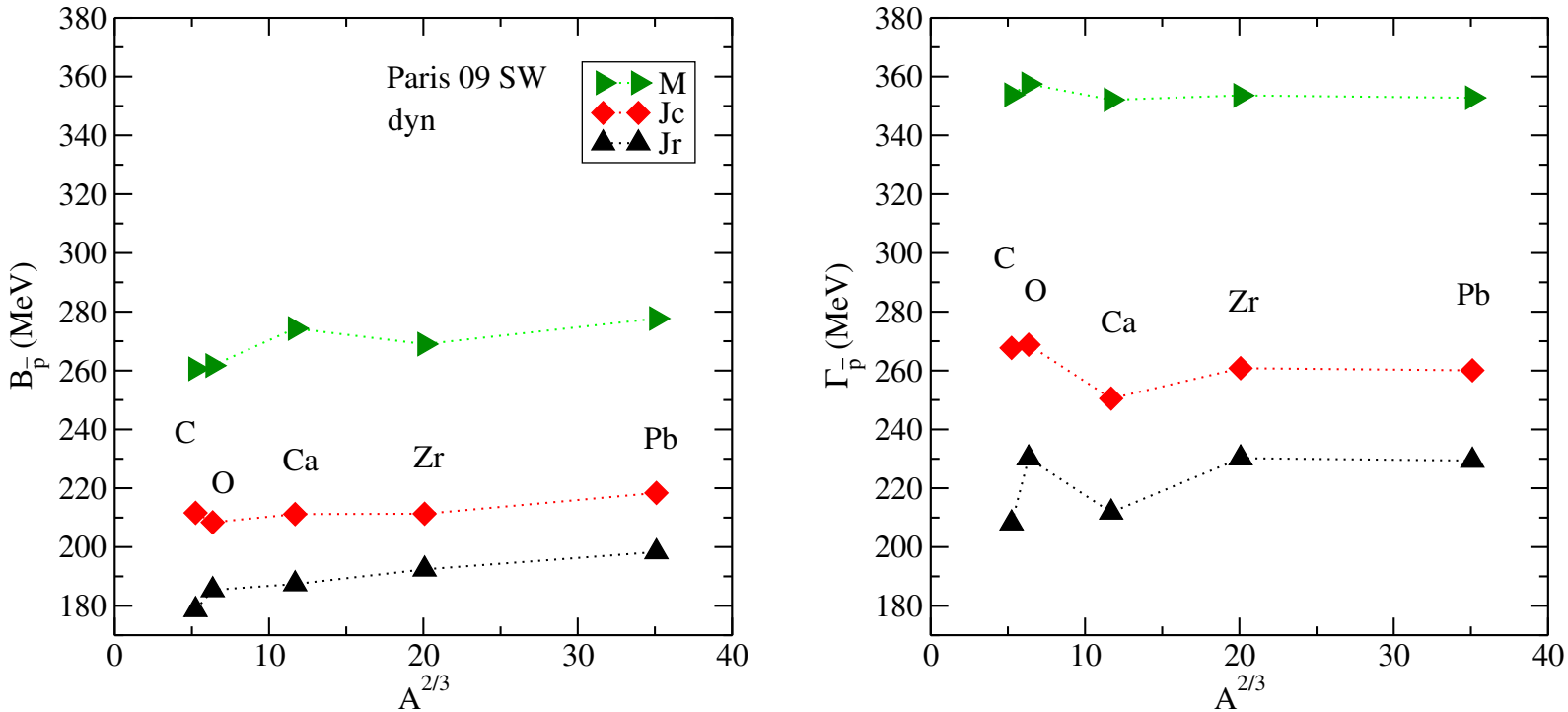

Fig.6: $1s$ $\bar{p}$ binding energies $B_{\bar{p}}$ (left) and widths $\Gamma_{\bar{p}}$ (right) in various nuclei, calculated dynamically with S-wave Paris amplitudes and different forms of $\sqrt{s}$.

S-wave Paris potential vs. phenomenological potential

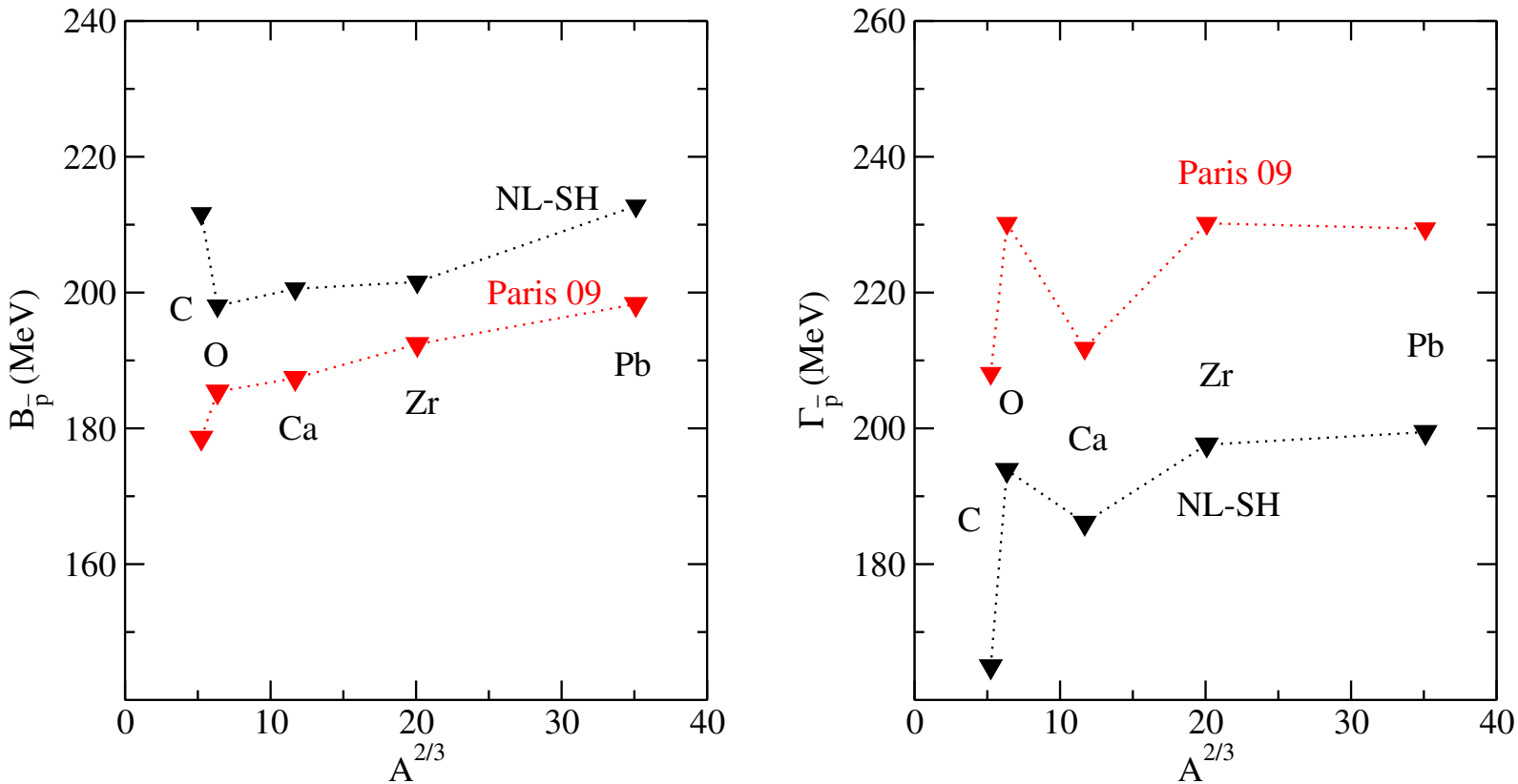

Fig.7: Binding energies (left panel) and widths (right panel) of $1s$ $\bar{p}$-nuclear states in selected nuclei, calculated dynamically for $\sqrt{s} =$ Jr using the Paris $\bar{N}N$ S-wave potential (red) and phenomenological approach within the RMF model NL-SH (black).

S-wave Paris potential vs. phenomenological potential

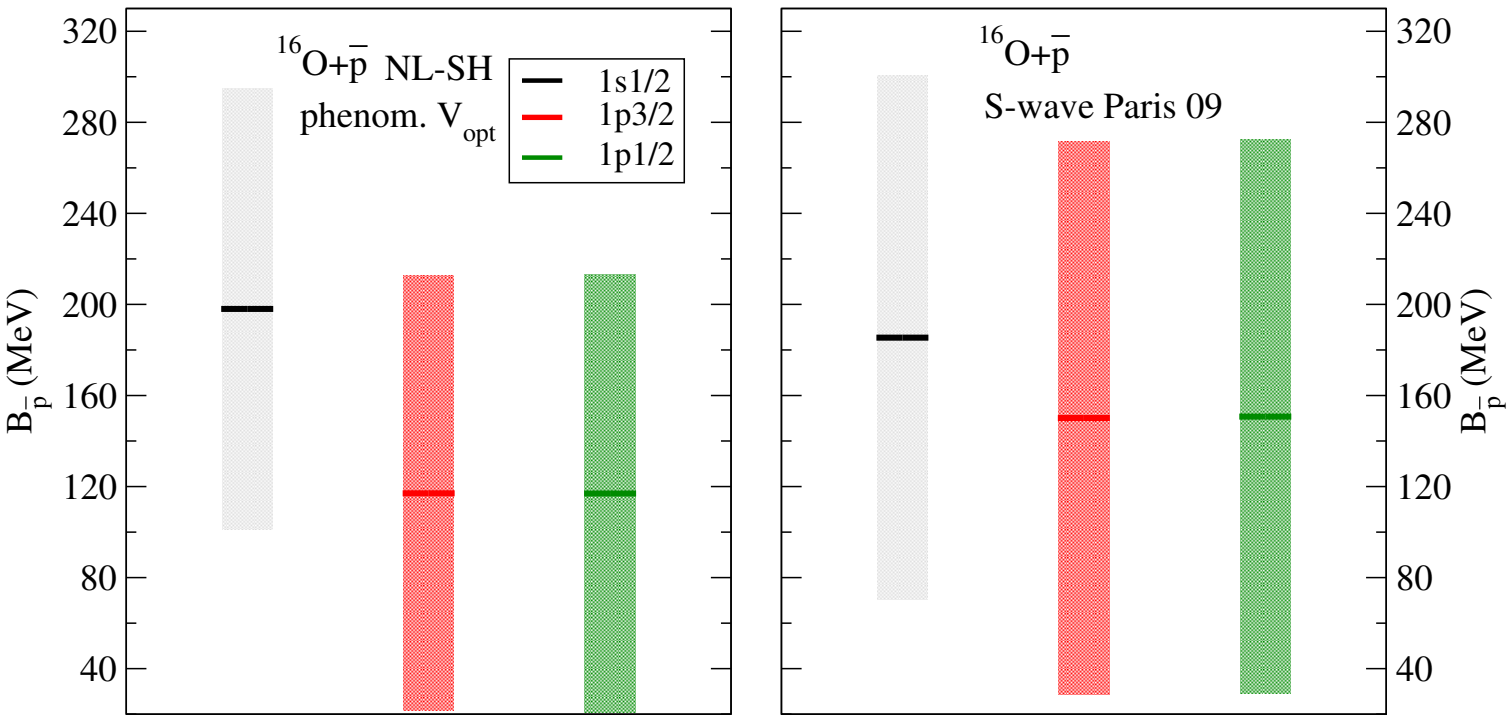

Fig.8: 1s and 1p binding energies (lines) and widths (boxes) of $\bar{p}$ in ^{16}O calculated dynamically within the NL-SH model for $\sqrt{s}$ = Jr with phenomenological $\bar{p}$ optical potential (left) and S-wave Paris potential (right).

P-wave interaction

- The P-wave potential

$$2E_{\bar{p}}V_{\text{opt}} = q(r) + 3\vec{\nabla}\cdot\alpha(r)\vec{\nabla}$$

where

$$\alpha(r) = 4\pi\frac{m_N}{\sqrt{s}}\left(f^P_{p\bar{p}}(\delta\sqrt{s})\rho_p + f^P_{n\bar{p}}(\delta\sqrt{s})\rho_n\right)$$

- $S + P$-wave Paris potential does not fit the $\bar{p}$ atom data
- S-wave Paris potential + phenomenological P-wave yield satisfactory agreement with the atom data

(*E. Friedman, A. Gal, B. Loiseau, S. Wycech, NPA 934 (2015) 101*)

Paris P-wave amplitudes

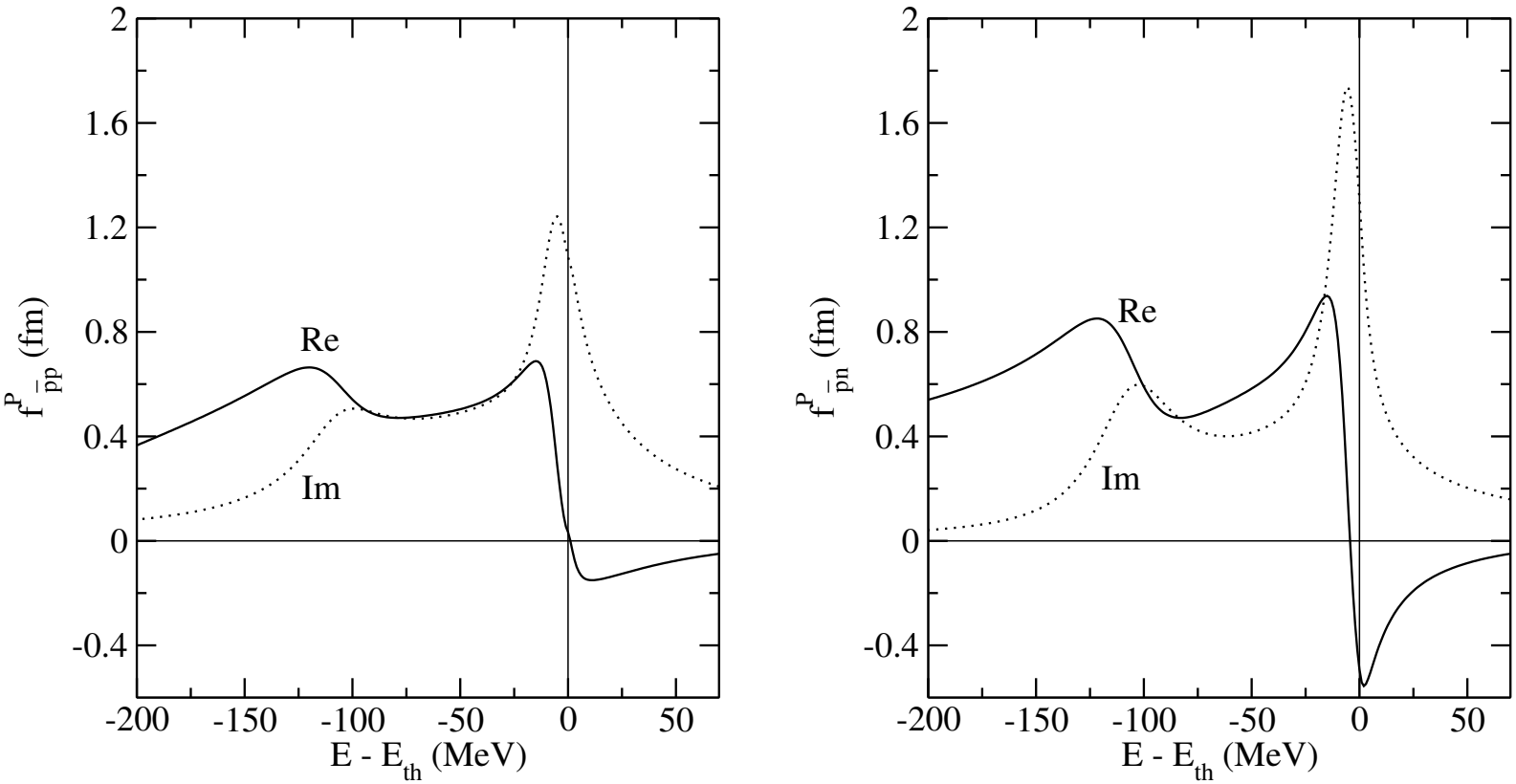

Fig.3: Energy dependence of the Paris 09 $\bar{p}p$ (left) and $\bar{p}n$ (right) P-wave free-space amplitudes.

P-wave interaction

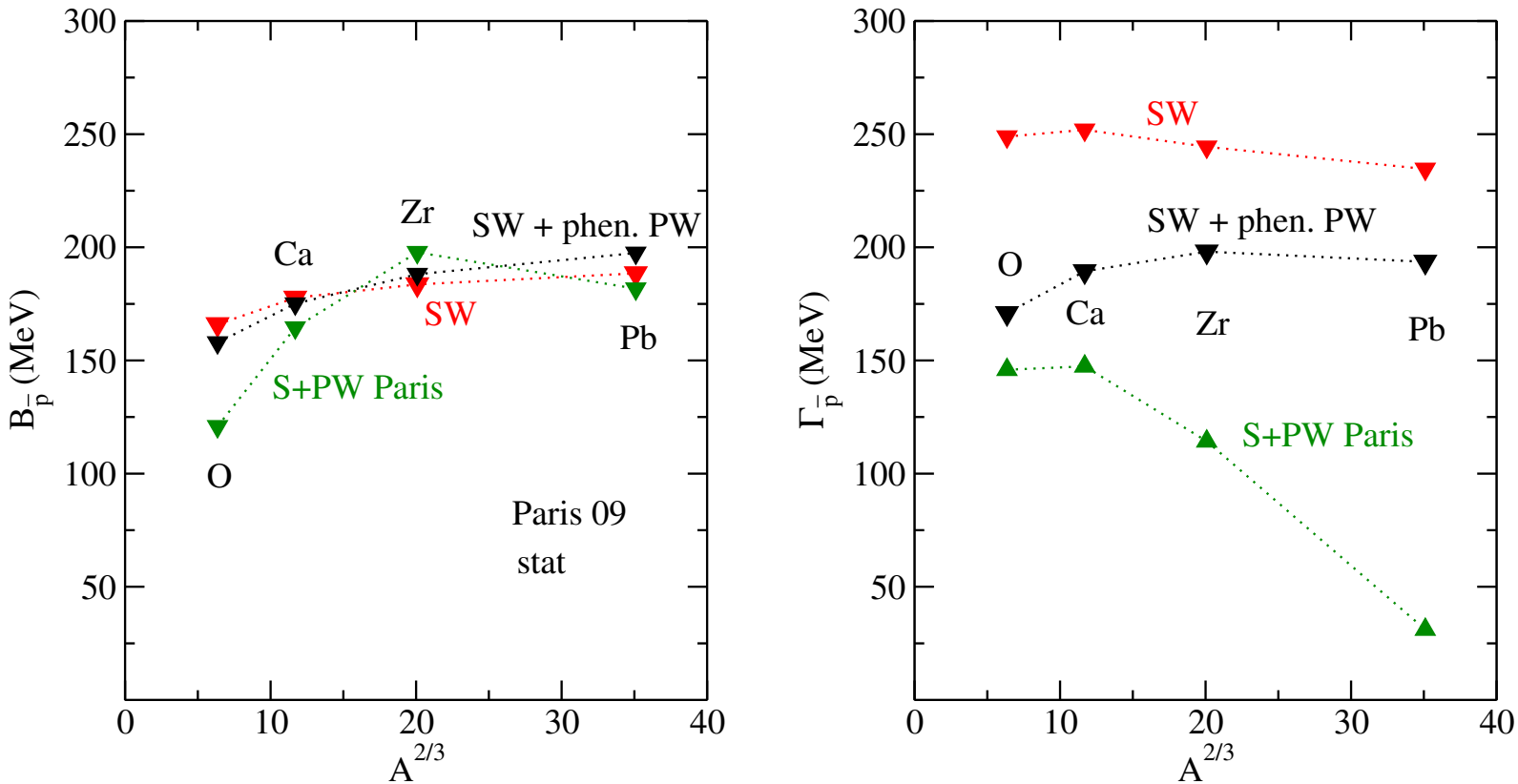

Fig.9: $1s$ $\bar{p}$ binding energies (left) and widths (right) in various nuclei, calculated statically with phenomenological P-wave potential (black), Paris P-wave potential (green) compared with only the Paris S-wave potential (red) for $\sqrt{s} =$ Jc.

P-wave interaction

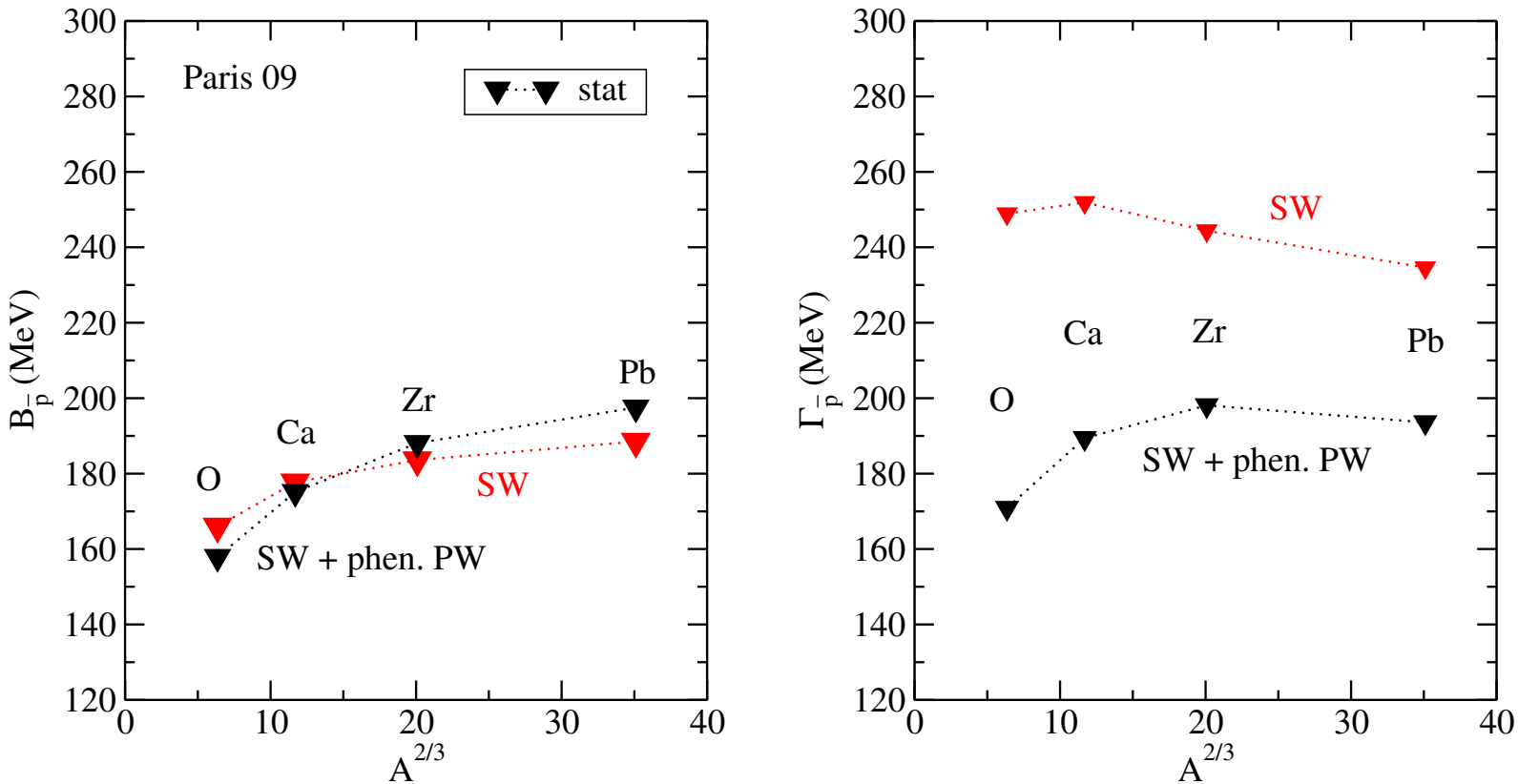

Fig.10: 1s $\bar{p}$ binding energies (left) and widths (right) in various nuclei, calculated statically with phenomenological P-wave potential (black) compared with only the Paris S-wave potential (red) for $\sqrt{s} =$ Jc.

P-wave interaction

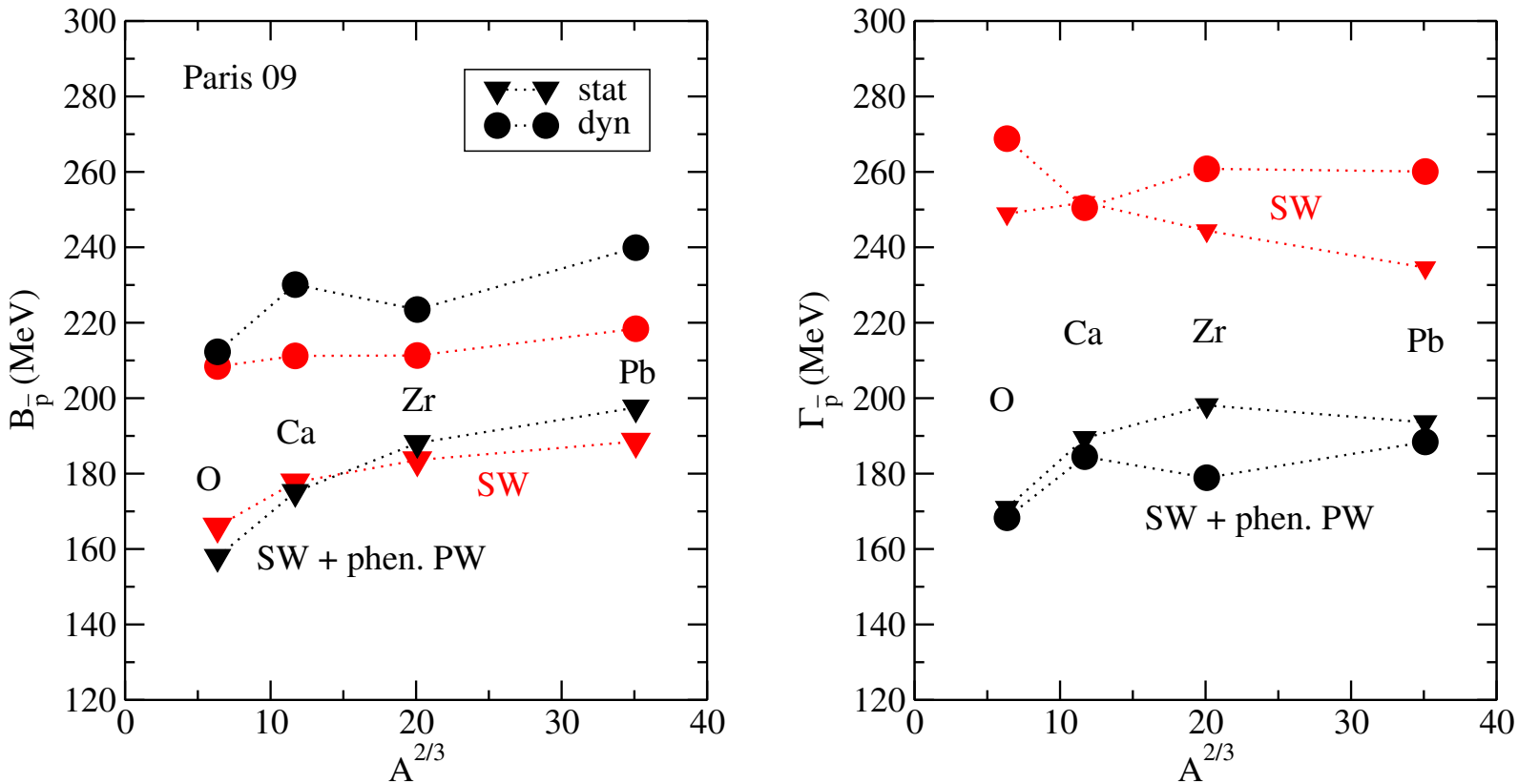

Fig.10: $1s$ $\bar{p}$ binding energies (left) and widths (right) in various nuclei, calculated statically and dynamically with phenomenological P-wave potential (black) compared with only the Paris S-wave potential (red) for $\sqrt{s} =$ Jc.

Conclusions

- calculations of $\bar{p}$ quasi-bound states in various nuclei with the Paris 09 $\bar{N}N$ potential
- the $\bar{p}$ potential is strongly energy dependent
- the S-wave Paris potential
  - yield comparable binding energies and larger corresponding widths than the phenomenological approach within the RMF model
    (*J. Hrtankova, J. Mares, NPA 945 (2016) 197)*
  - dynamical effects are not so pronounced $\sim 25\%$
- the P-wave interaction considered — Paris vs. phenomenological
  - Paris P-wave interaction yields too small widths in heavy nuclei
    (also fails to reproduce $\bar{p}$ atom data)
  - phenomenological P-wave interaction slightly increases the $\bar{p}$ binding energies and decrease the $\bar{p}$ widths
  - the $\bar{p}$ widths are still sizable

Thank you for your attention!